Supporting Information

Bio-Inspired Dumbbell-Shaped Nanochannel with Controllable Structure and Ionic Rectification

Kai Xiao, Lu Chen, Ganhua Xie, Pei Li, Xiang-Yu Kong, Liping Wen, and Lei Jiang*

1. **Fabrication of symmetric dumbbell-shaped nanochannel**
2. **Electrochemical testing setup and conditions**
3. **Electrolytes conductivities**
4. **Ions selectivity**
5. **Current-voltage properties**
6. **Targeted surface modification**
7. **Surface properties under asymmetric electrolyte solutions**
8. **Model calculation by Poisson–Nernst–Planck (PNP) theory**

1. Fabrication of symmetric dumbbell-shaped nanochannel

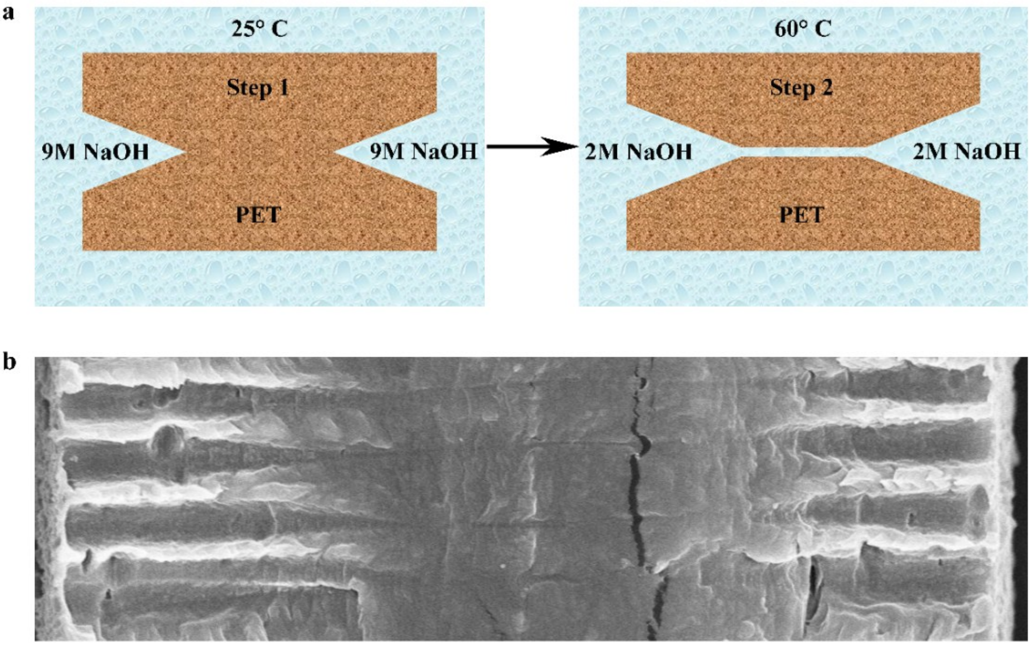

Figure S1. Schematic of the symmetric dumbbell-shaped nanochannels fabrication and cross sections of the dumbbell-shaped nanochannels. a) The etching process is based on the low-high-temperature collaborative two-step method. b) Cross sections of the dumbbell-shaped nanochannels ($\lambda_{0.28}$).

The fabrication of nanochannels in 12 μm thick PET films was performed by the track-etching technique. Polymer films of polyethylene terephthalate (PET) of 12 μm thickness were irradiated at the linear accelerat or UNILAC (GSI, Darmstadt) with swift heavy ions (Pb , U, and Au) having an energy of 11.4 MeV pernucleon. After irradiating the films with energetic ions, both sides of the membranes were treated with UV light for 2 h. Subsequently, the film was placed between two halves of a conductivity cell. To produce a dumbbell-shaped nanochannel, etching was performed from both sides. The following are the etching and stopping solutions (**Figure S1 a and Table S1**). First step: 9 M NaOH for etching at 25° C; Second step: 2 M NaOH for etching at 60° C, then1 M KCl + 1 M HCOOH for stopping. For the observation etching process, the voltage (1 V) used to monitor the etching process was applied in such a way that the transmembrane ionic current can be observed as soon as the nanochannel opened. To both sides of the cell were added a solution that is able to neutralize the etchant as soon as the nanochannel opens, thus slowing down the further etching process. After etching, the cross sections of the channel can be gotten by field emission scanning electronmicros (SEM) (**Figure S1 b**). Specifically, the membrane was put into liquid nitrogen for 10 min, then the membrane was snapped quickly, which can prevent the stretching strain and protect the original morphology. Then, the length of cylindrical segment was measured by analyzing the SEM images of the dumbbell-shaped nanochannels with different etching conditions (Figure 1b), which can be measured directly by image manipulation software. To a specific symmetric geometry degree λ, at least 10 nanochannels etched in same conditions were analyzed to get the average length of cylindrical segment.

Table S1. The relationship between morphology and etching conditions.

λ	Etching Time (9 M NaOH)	Etching Time (2 M NaOH)	Length of conical segment	Length of cylindrical segment
1.0	0 min	4 min	0 μm	12 μm
0.72	8 min	3 min	1.7 μm	8.6 μm
0.45	16 min	2 min	3.3 μm	5.4 μm
0.28	24 min	1 min	4.3 μm	3.4 μm
0	30 min	0 min	6 μm	0 μm

2. Electrochemical testing setup and conditions

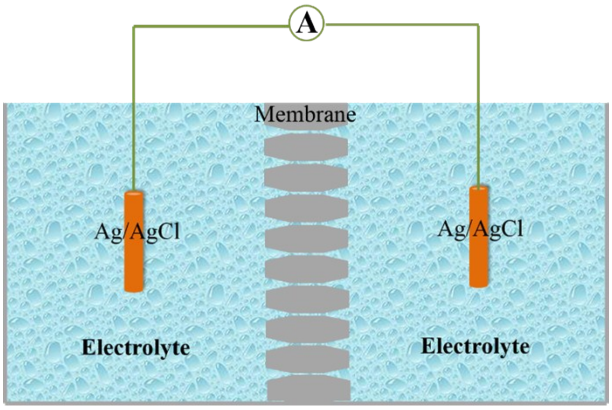

Figure S2. Schematic of the electrochemical testing setup.

In our experiment, the set-up device is shown in detail as Figure S2. The ionic current was measured by a Keithley 6487 picoammeter (Keithley Instruments, Cleveland, OH). The nanochannel-membrane was mounted between two halves of a conductivity cell; and each half cell was filled with electrolyte of 0.1 M KCl aqueous solution with different pH values. The pH of electrolyte can be adjusted by hydrochloric acid and sodium hydroxide solutions. Ag/AgCl electrodes were used to apply a transmembrane potential, and the scanning voltage varied from -2 V to +2 V with its period of 21 seconds. The pH of electrolyte can be adjusted by hydrochloric acid and sodium hydroxide solutions.

3. Electrolytes conductivities

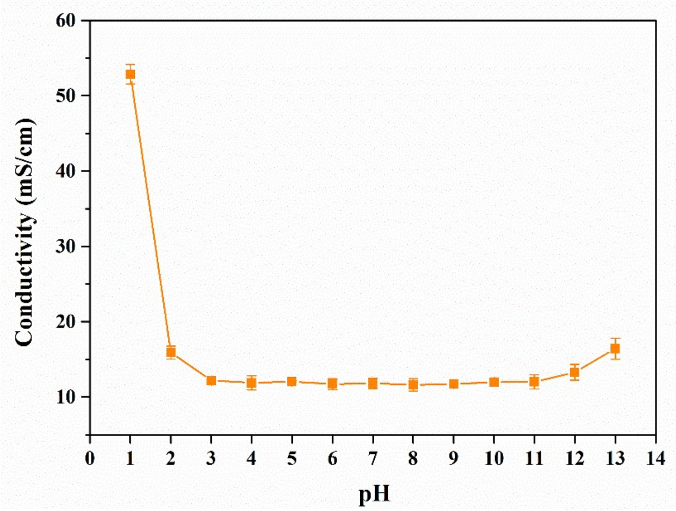

Figure S3. The electrolytes conductivities under different pH from 1 to 13.

In this experiment, different pH electrolytes, which was adjusted by hydrochloric acid and sodium hydroxide solutions, has no obvious influence to our results. The H^+ or OH^- ions may contribute to the total observed ionic current under pH 3 and 10, but a negligible effect because of the low concertation. We measured the electrical conductivity of the electrolyte with different pH from 1 to 13 under room temperature (Figure S3). It can clearly find that there are no significant difference of the electrical conductivities of electrolytes from pH 3 to 11 (about 12.2 mS/cm). Under pH 3, the H^+ ion concertation is about 0.001M/L while the OH^- ions concertation is about 0.0001M/L under pH 10. Compared with the 0.1 M/L KCl electrolyte, the H^+ or OH^- ions concertation is too small and always neglected in the testing process.

4. Ions selectivity

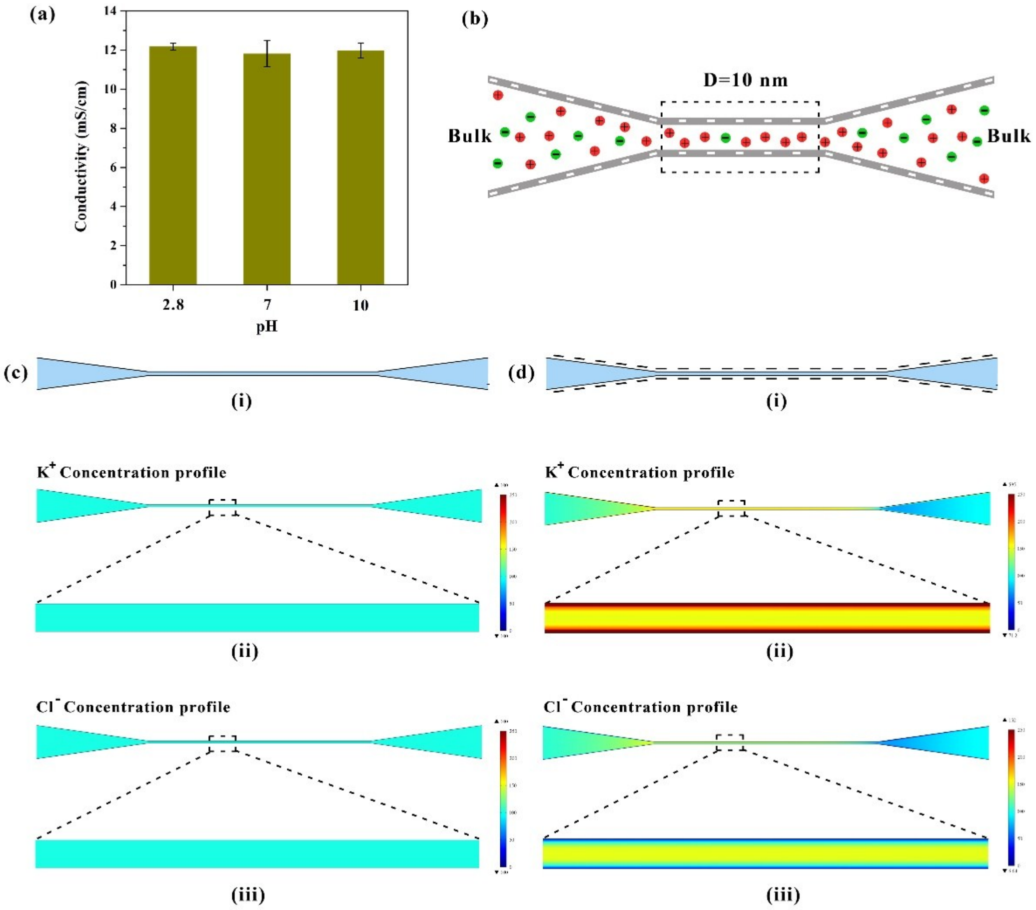

Figure S4. (a) The electrical conductivities of the electrolytes under pH 2.8, 7, and 10. (b) Surface charge effects in nanochannels. (c) The K^+ ions and Cl^- ions concentration profiles show no difference with bulk when the nanochannel is electroneutral. (d) The K^+ ions and Cl^- ions concentration profile is larger than bulk concentrations while the K^+ ions is several times the concentration of Cl^- ions.

We measure the electrical conductivities of the electrolytes with pH 2.8, 7, and 10 (**Figure S4 a**). It can be clearly find that there is no significant difference with pH 2.8, 7, and 10, which indicate that the difference in ion current through the channels at pH 2.8 and pH 10 is not from the differences in conductivity of the electrolyte, but from the ion selectivity of the charges nanochannel.

In addition, previous study has shown that the solution is charged when the Debye length is larger than the channel dimensions in a nanochannel because the charged channel surface would adsorb the counter-ions in the electrolyte. Thus, the counter-ion concentration (K$^+$ ions, red) in a nanochannel is much higher than the co-ion concentration (Cl$^-$ ions, blue) (**Figure S4 b**). Our numerical simulation also showed that the K$^+$ ions concentration has no difference with the Cl$^-$ ions concentration (equal to bulk) when the dumbbell-shaped nanochannel is electroneutral. When the nanochannel is negative charged, both the K$^+$ and Cl$^-$ ions concentrations are higher that the bulk concentrations (**Figure S4 c, d**), which can explain the larger ion current under pH 10. Meanwhile, the K$^+$ ions is several times the concentration of Cl$^-$ ions (**Figure S4 d ii, iii**), which can prove that the negative charged nanochannel is cation (K$^+$) selectivity and agree with our experimental. This information can be found in the revised manuscript. The detailed numerical simulation can be found in section 8.

5. Current–voltage properties

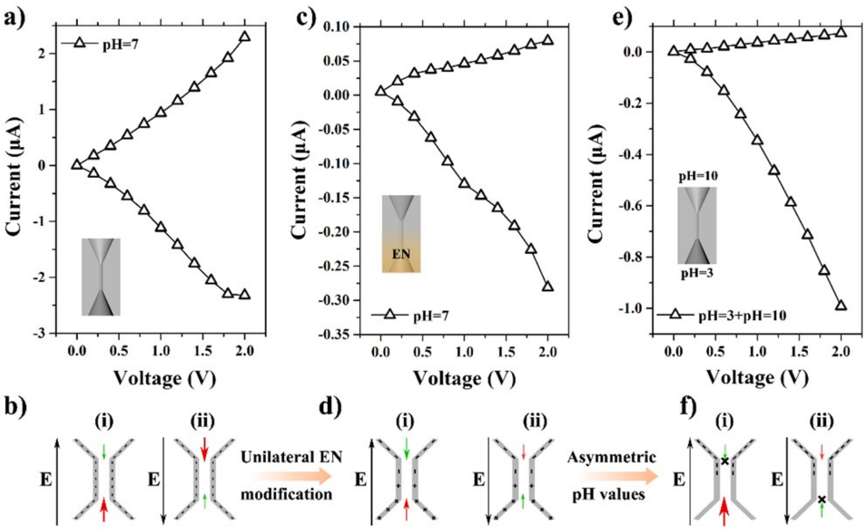

Figure S5. a) Current–Voltage properties of the symmetric dumbbell-shaped nanochannel (λ=0.45) recorded under pH 7. b) Explanation of the Bidirectional ion selectivity under ±2 V. c) Current–Voltage properties of the symmetric dumbbell-shaped nanochannel (λ=0.45) recorded under pH 7 after unilateral EN modification. d) Explanation of the unidirectional ion selectivity under ±2 V. e) Current–Voltage properties of the symmetric dumbbell-shaped nanochannel (λ=0.45) recorded under asymmetric pH. f) Explanation of the ion rectification under ±2 V.

Figure S5 a exhibited symmetric ion transportion of the dumbble-shaped nanochannel under pH 7. The dumbbell-shaped nanochannel showed no selectivity difference of the anion (Cl$^-$) and cation (K$^+$) under pH 7 due to the uniformity of the symmetric geometry and symmetric surface charge under ±2 V (**Figure S5 b**). After unilateral EN modified, the ion selectivity from bidirectionally to unidirectional can be obtained ascribed to the effect of asymmetric surface charge under varied symmetric electrolyte solutions (**Figure S5 c, d**). The unmodified dumbbell-shaped nanochannel also can rectified ionic current at asymmetric electrolyte condition because asymmetric surface charge also can be generated in these conditions (**Figure S5 e, f**).

6. Targeted surface modification

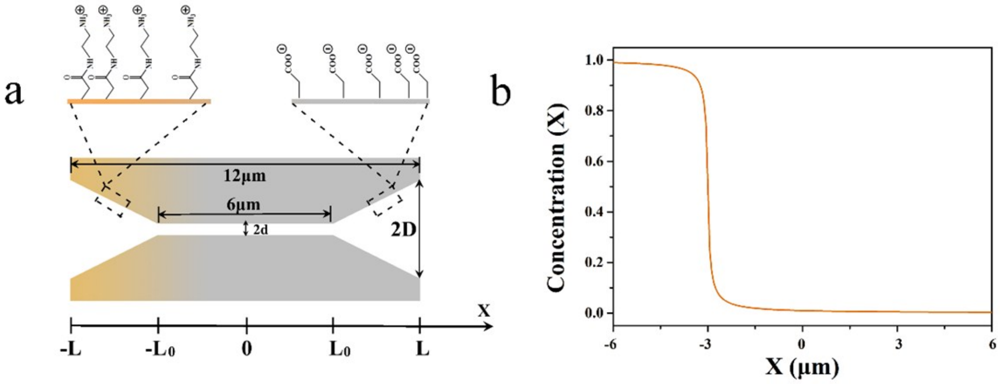

Figure S6. Steady-state distribution of EN placed only on the conical segment of the dumbbell-shaped nanochannel. a) Scheme of the distribution of amino groups and carboxyl groups on the surface. b) Surface densities of amino groups calculated from eq 1 after 30 min of modification.

The asymmetrical distribution of the amino groups and carboxyl groups is achieved by placing reagent only on the one side of the dumbbell-shaped nanochannels because the main advantage of the dumbbell-shaped nanochannel is the non-homogeneity of the distribution of the chemical introduced from only one side if the channel along channel's centerline. There is a very steep decrease of the concentration in the channel where the spout is located. (**Figure S6**) This assures a high concentration at one side of the nanochannel where the chemical of interest is, and basically zero concentration at the other side of the dumbbell-shaped nanocahnnel.

$$\mathrm{c}(x)=\begin{cases} c_0\cdot(\frac{1}{2}\cdot\frac{d\cdot L}{(x+L_0)\cdot D-d\cdot L}+1) & -\mathrm{L}<\mathrm{X}<-\mathrm{L}_0 \\ c_0\cdot\frac{1}{2}\cdot\frac{d\cdot L}{(x+L_0)\cdot D+d\cdot L} & -\mathrm{L}_0<\mathrm{X}<\mathrm{L} \end{cases} \qquad \text{Equation 1}$$

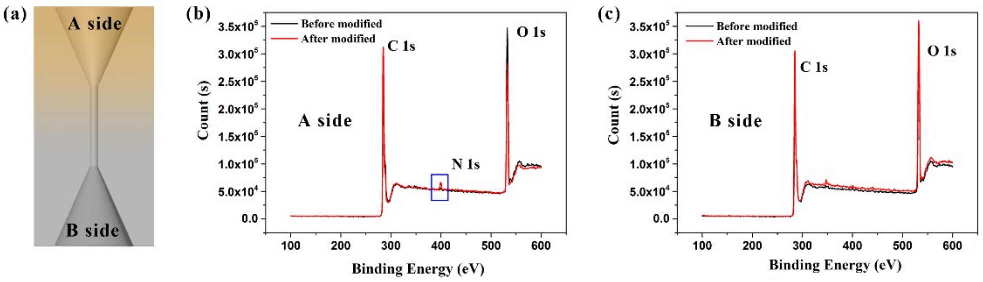

Figure S7. (a) Schematic diagram of the unilateral modified nanochannel. (b) XPS spectra of ethylenediamine-modified A side of the membrane. (c) XPS spectra of unmodified B side of the membrane.

The XPS information of two sides of the dumbbell-shaped nanochannel before and after modification were shown in **Figure S7**. The binding energies were referenced to the C1s line at 284.8 eV from adventitious carbon. In our experiment, A side was modified with EN while B side was to do no processing (**Figure S7a**). It can be clearly found that the there is only "C1s" and "O1s" peaks in the unmodified membrane (**Figure S7b, c** black line). After ethylenediamine modification, there is an obvious peak near 400 in A side (**Figure S7 c** red line), which indicating a typical "N1s". In the B side, it is the same with unmodified membrane. These result can clearly indicated that ethylenediamine was only immobilized on the A side of the PET membrane. These result also can be found in the revised supporting information.

7. Surface properties under asymmetric electrolyte solutions

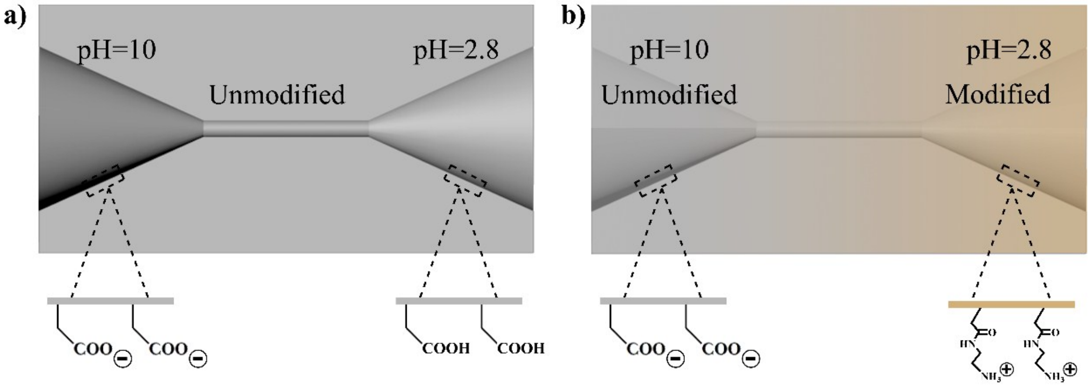

Figure S8. Corresponding surface properties of the nanochannel under asymmetric pH condition.

Under asymmetric pH condition, the unmodified dumbbell-shaped nanochannel exhibited negative charged in the side of pH 10 while electroneutral in the side of pH 2.8 (**Figure S8 a**). The unilateral modified dumbbell-shaped nanochannel exhibited patterned surface charge with negative charged in the side of pH 10 and positive charged in the side of pH 2.8 (**Figure S8 b**).

8. Model calculation by Poisson–Nernst–Planck (PNP) theory

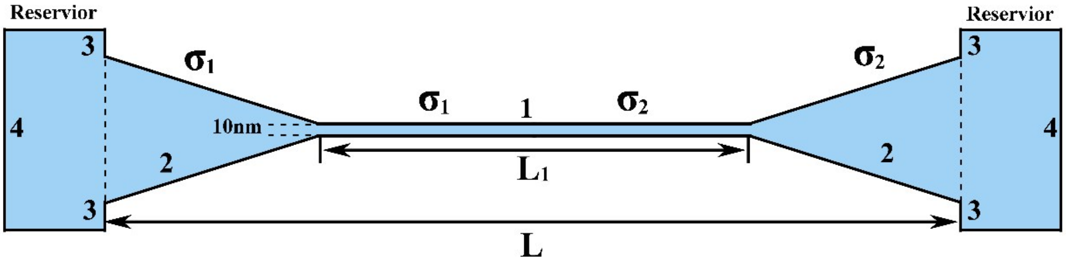

Figure S9. Sketch of the computation domain for the dumbbell-shaped nanochannel. Two electrolyte reservoirs are connected by the dumbbell-shaped nanochannel. Both the outer and inner surface of the nanochannels are charged. The ionic concentration in both reservoirs is 0.1 M.

The set of coupled equations was solved using the commercial software COMSOL Multiphysics 4.4. The multiphysics mode proved to be extremely useful for our purpose because it readily allows solutions of the coupled governing equations for arbitrary geometry. And the sketch of the computation domain for the dumbbell-shaped nanochannel is shown in **Figure S9**. The dumbbell-shaped nanochannel is symmetric along the axis of the channel. Total length of all simulated models was uniformly set to be 12 μm. In addition to considering charge on the wall of the nanochannel, the influence of charge on the surface exterior to the channel orifice (surface 3) was also included. It is important to include the effect of charge on this external surface in modeling transport through nanochannels in polymer membranes, as this surface has the same chemistry as the interior wall of the nanochannel. Two surfaces (surface 4) correspond to the electrodes used to apply a bias voltage across the nanochannel. These surfaces are held at constant potential, with one in the reservoir designated as ground. The concentration of electrolyte at these surfaces is held constant at the bulk value. An adaptive mesh refinement was used to optimize the mesh size geometry. The adjustment algorithm refined the mesh at the charged wall down to a value of 0.6 nm, sufficient for accurately resolving the features of the electric double layer.